Using Atmospheric Radiation Measurement Data to Evaluate Satellite Surface Solar Flux Retrievals

L.M. Hinkelman
National Institute of Aerospace
Hampton, Virginia

P.W. Stackhouse and D.F. Young
National Aeronautics Space Administration, Langley Research Center
Hampton, Virginia

C.N. Long
Pacific Northwest National Laboratory
Richland, Washington

D. Rutan
Analytical Services and Materials, Inc.
Hampton, Virginia

Introduction

The accurate, long-term radiometric data collected by the Atmospheric Radiation Measurement (ARM) Program is essential to evaluating surface radiation budget data from satellites. Because the spatial and temporal characteristics of data from these two sources are different, the comparisons are typically made for long-term average values. While such studies provide a general indication of the quality of satellite flux products, more detailed analysis is required to understand specific retrieval algorithm weaknesses. Here we show how data from the ARM Shortwave Flux Analysis (SFA) Value-Added Product (VAP) are being used to assess solar fluxes in the Global Energy and Water Cycle Experiment (GEWEX) Surface Radiation Budget (SRB), release 2.5.

Method

The shortwave (SW) components of the GEWEX SRB are computed at 3-hour intervals on a nominally 1°global grid by applying the algorithm of Pinker and Laszlo (1992) to International Satellite Cloud Climatology Project (ISCCP) cloud and radiance data. For this analysis, we compare data from the ARM Southern Great Plains (SGP) Central Facility to output for the closest SRB grid box. As shown in Figure 1, the Central Facility falls near the center of this grid box.

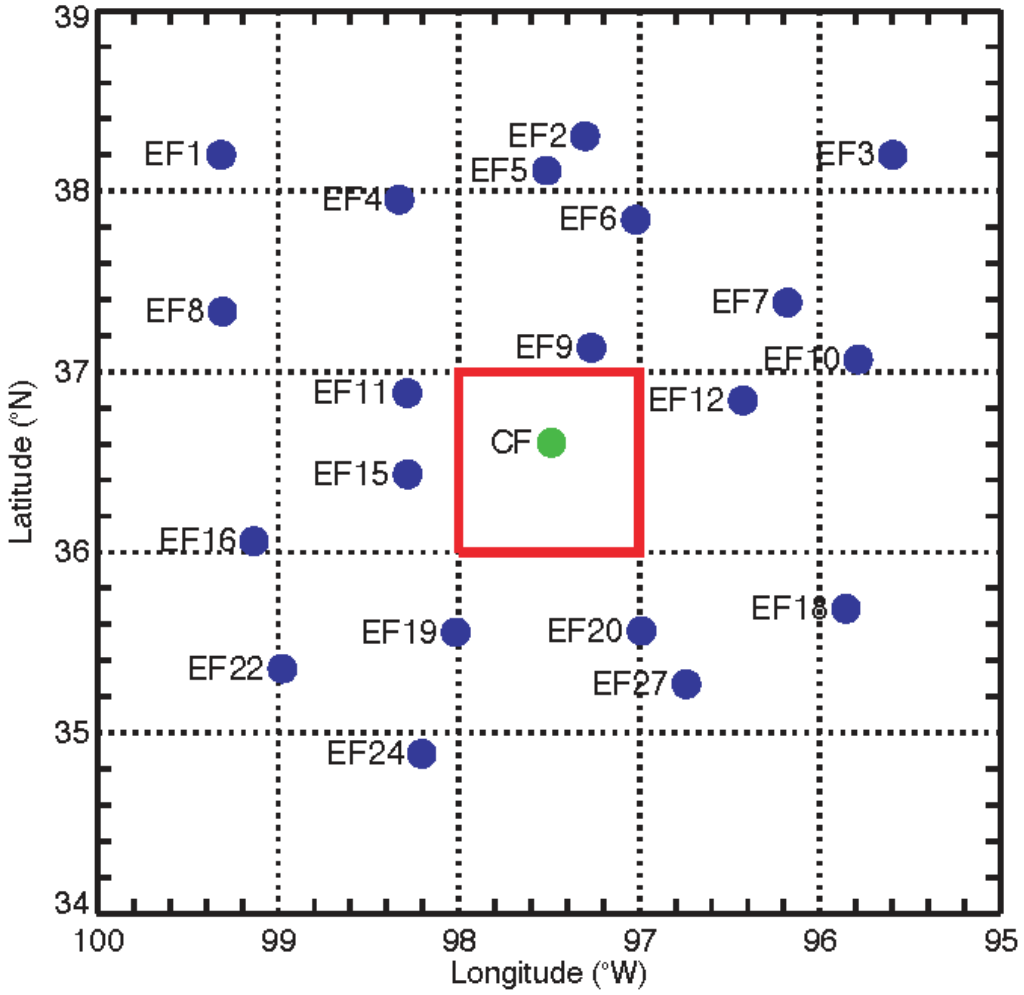

Figure 1. Map of the ARM SGP site. The SRB grid box used in this study is indicated in red. (CF = Central Facility, EF = extended facility.)

A typical validation plot for the SRB downwelling SW surface flux is shown in Figure 2. Here, monthly mean values for the period of July 1998 through September 2001 are compared to measurements from the SGP Central Facility. The values agree well except for a slight negative bias in the SRB product.

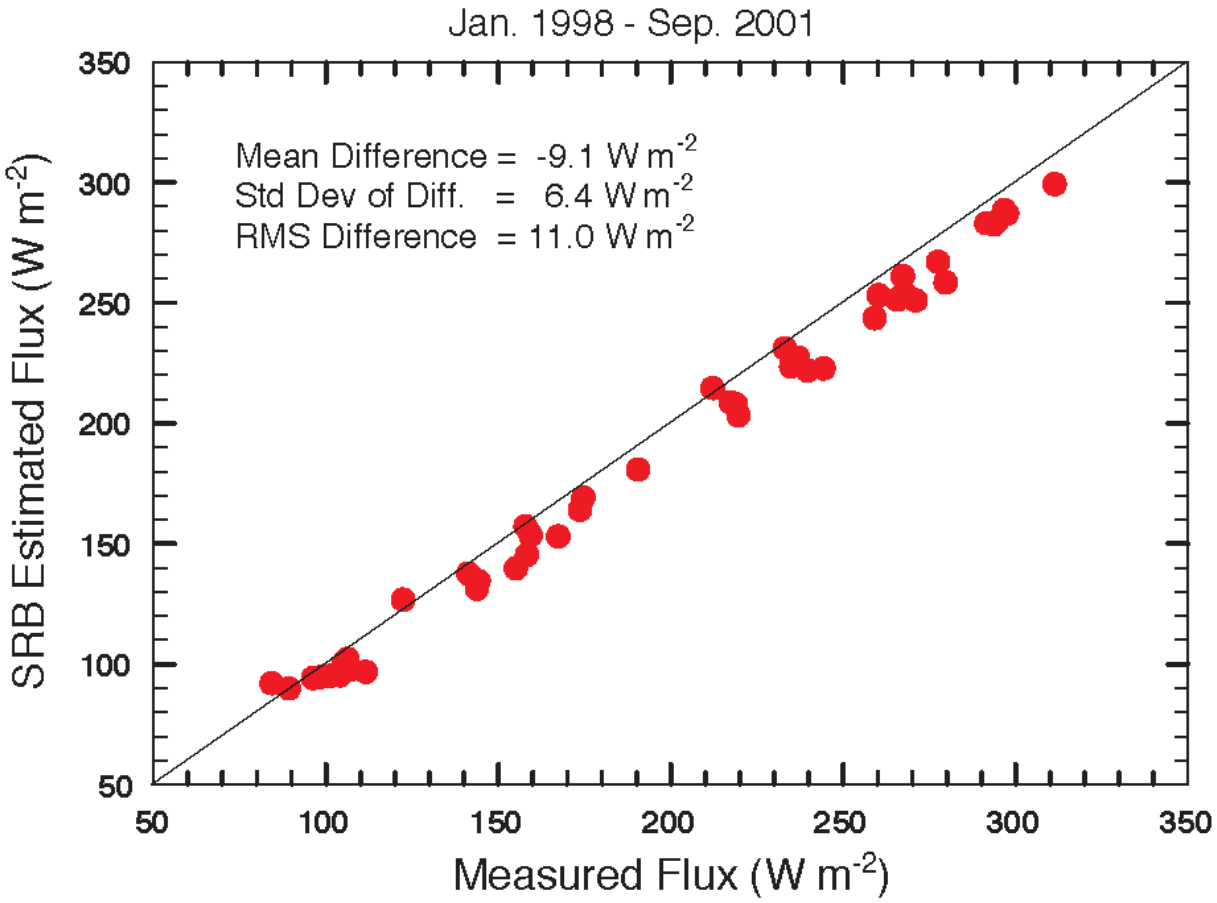

Figure 2. Comparison of SRB and ARM monthly mean SW total fluxes for 1998 through 2001.

In order to determine the source of this bias, we make a detailed comparison of individual instantaneous SRB fluxes with 60-minutes averages from the ARM site. As a diagnostic aid, the sky cover at each time is first classified according to statistics of the total SW flux measured at the surface divided by the expected clear-sky flux from the Long-Ackerman algorithm (Long and Ackerman 2000). The mean of this parameter over 60 minutes gives an indication of the total cloud amount, while the variance corresponds to brokenness. The sky cover classification scheme is illustrated in Figure 3.

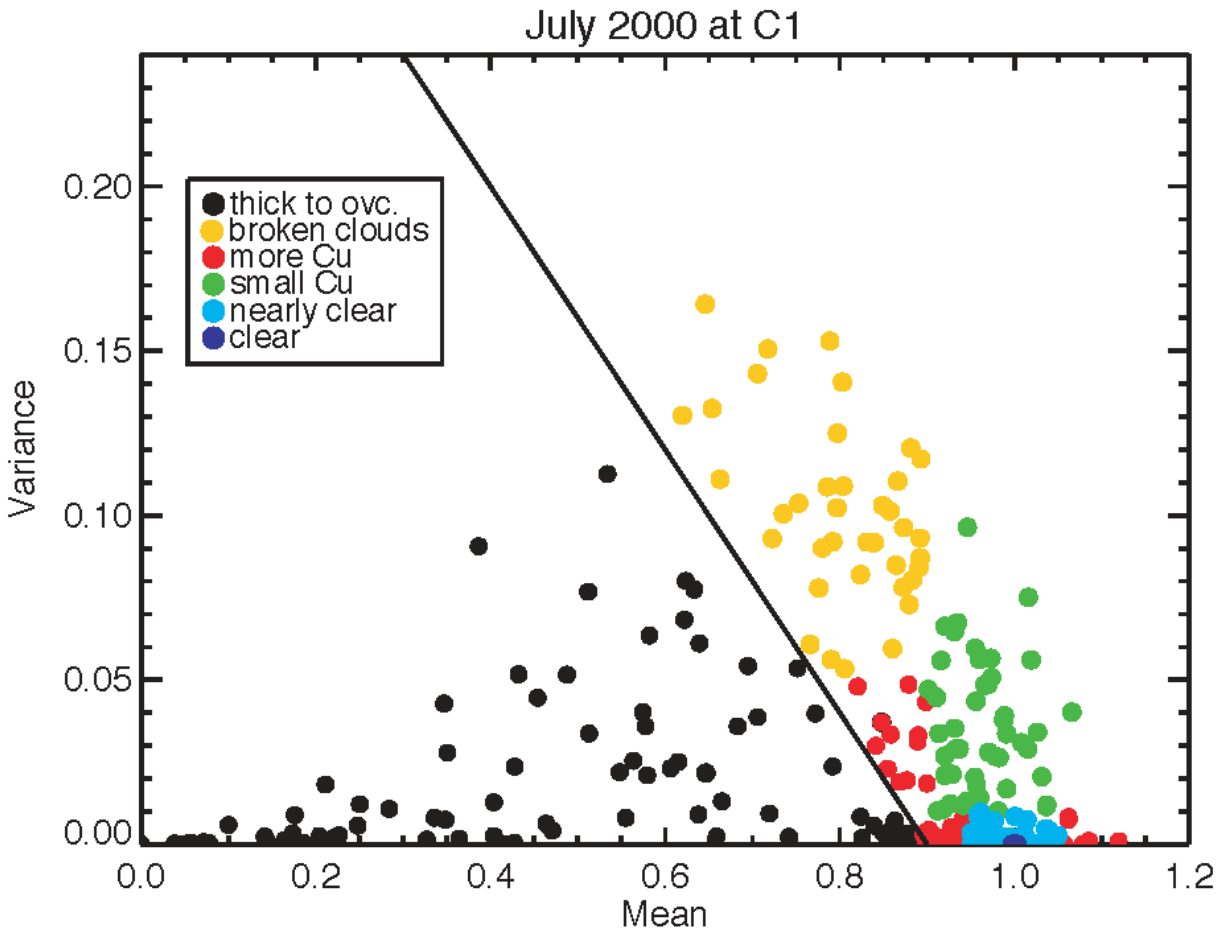

Figure 3. Sky-cover classification scheme based on statistics of the measured downwelling SW flux normalized by the expected SW clear-sky flux from the Long-Ackerman algorithm. (C1 is the SGP Central Facility.)

Results

The total downwelling shortwave fluxes at different times of the year 2000-2001 are compared in Figure 4. (Hours for which the average cosine of the solar zenith angle is less than 0.1 are omitted.) For the months shown, the root mean square (RMS) difference between the retrieved and measured values varies only slightly, but the mean difference is significantly lower in July. The greatest flux differences occur under broken cloud conditions, although significant differences sometimes occur for overcast or nearly clear skies.

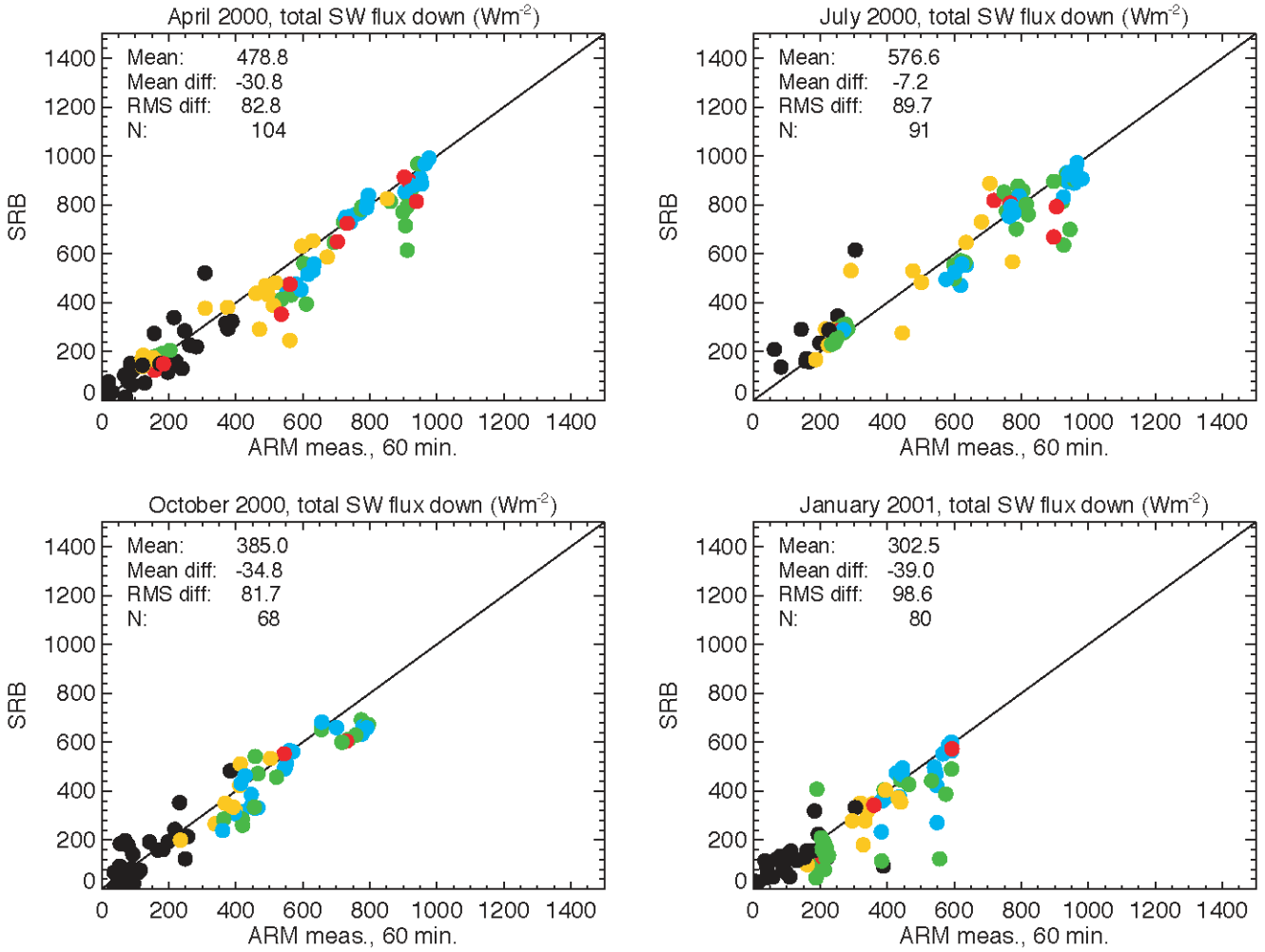

Figure 4. Comparison of retrieved and measured total downwelling SW flux at the surface with color coding for sky conditions as shown in Figure 3.

A plot of the same data normalized by the computed downward flux at the top of the atmosphere (TOA) in Figure 5 lends confidence to the sky-cover classification scheme, since transmittance is shown to increase with decreasing cloud cover. At the same time, it becomes evident that the largest relative differences between the retrieved and measured fluxes for these months occur in January.

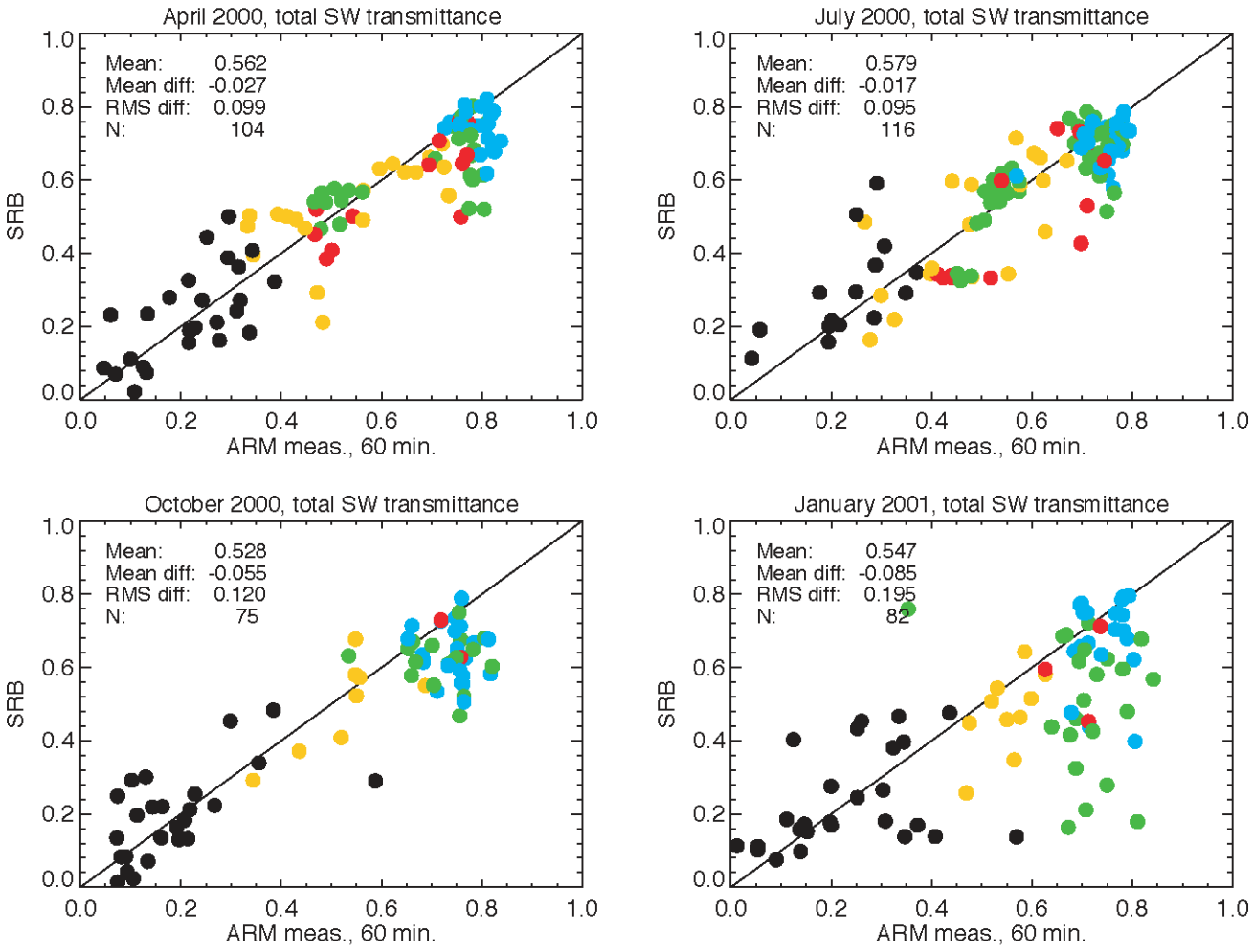

Figure 5. Comparison of retrieved and measured total SW transmission with color coding for sky conditions as shown in Figure 3.

Because the Pinker algorithm computes direct and diffuse SW fluxes independently, it is instructive to separately compare these terms to the corresponding measured values separately. Results of this comparison are given in Figure 6. This comparison reveals that, during the months studied, nearly all of the SRB direct flux values are lower than the surface measurements while the satellite-retrieved diffuse fluxes are high.

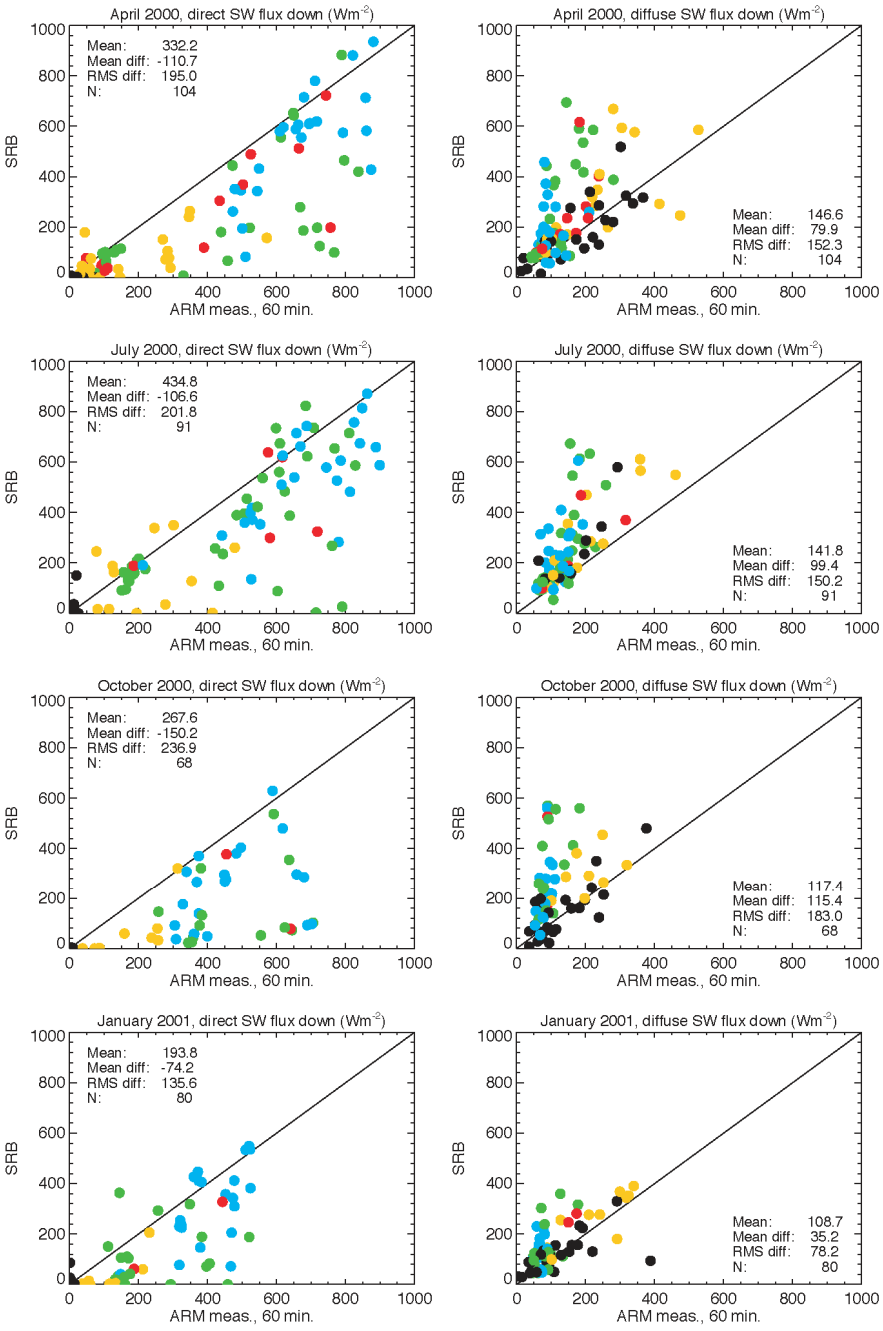

Figure 6. Comparison of retrieved and measured direct and diffuse components of the downwelling SW flux at the surface with color coding for sky conditions as shown in Figure 3.

As shown in Figure 7, comparison of the sky cover estimated by the SFA VAP at the ground site to the ISCCP cloud fraction used in the satellite retrieval explains the large differences observed for the direct and diffuse fluxes: the ISCCP cloud fractions are consistently higher than the sky cover detected at the surface in the months studied.

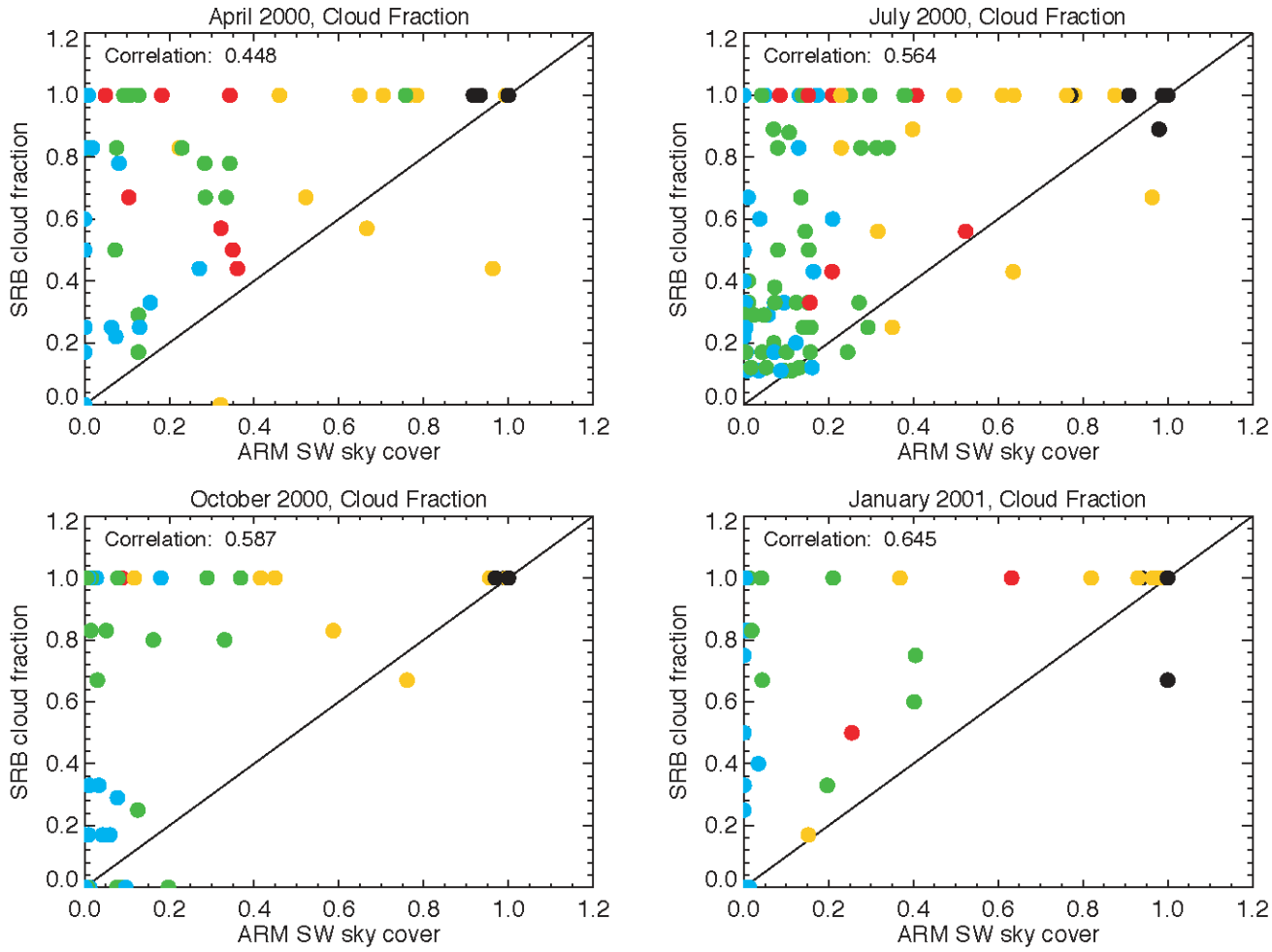

Figure 7. Comparison of ISCCP cloud fractions used in the SRB flux retrievals with sky cover from the SFA VAP. (Color coding for sky conditions as shown in Figure 3.)

Figure 8 indicates that larger flux differences tend to correlate with large cloud fraction differences, as would be expected. Again, some of the largest differences occur for skies perceived as broken from the surface site. This suggests that either ISCCP overestimates cloud amounts or that the cloud cover observed by the surface radiometer is not representative of the 1° SRB grid box.

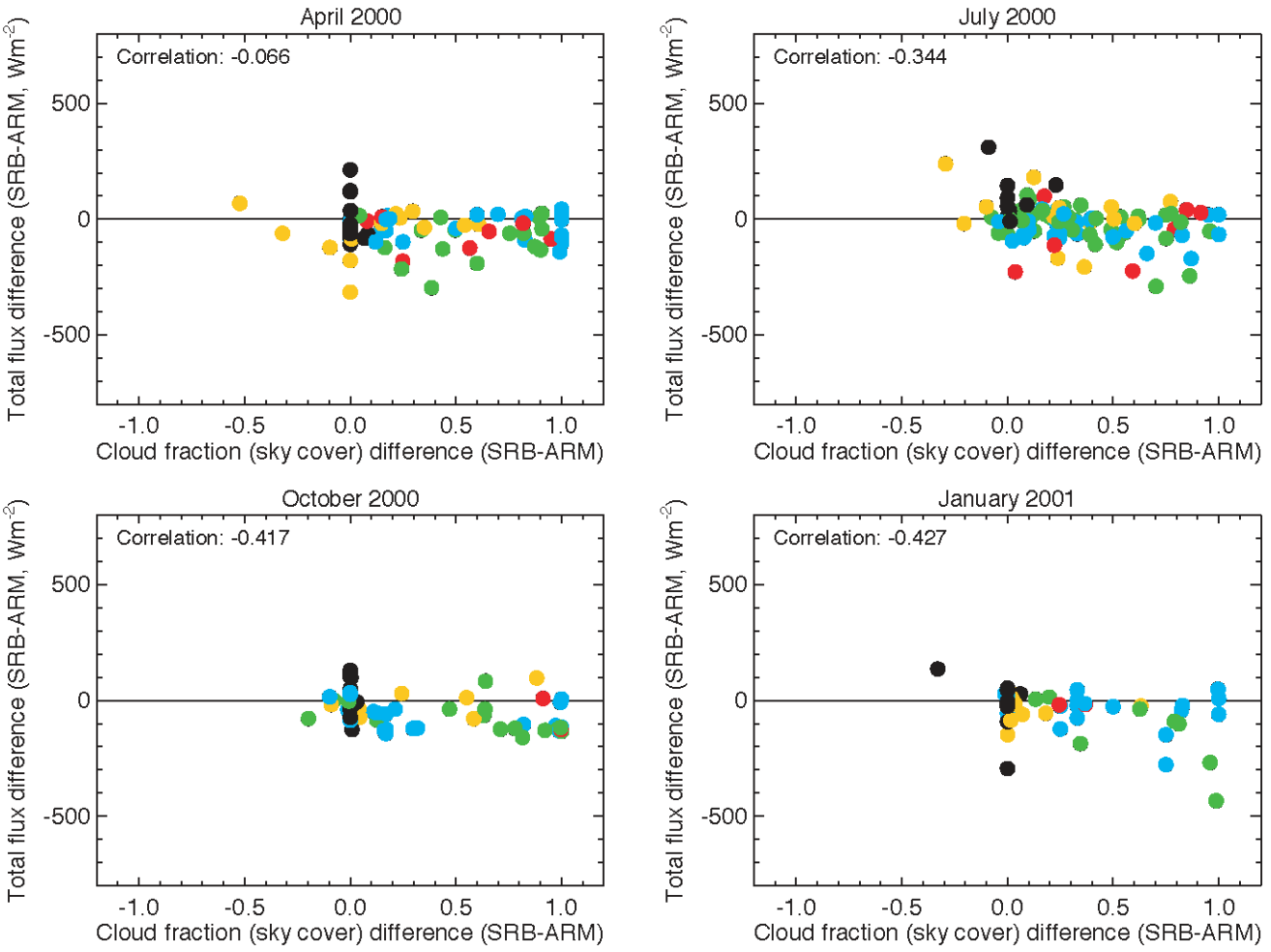

Figure 8. Differences between SRB and ARM total downwelling SW fluxes as a function of differences in detected sky cover. (Color coding for sky conditions as shown in Figure 3.)

Separate comparisons of the direct and diffuse flux differences as a function of sky cover difference explain the overall flux bias trends. As shown in Figure 9, the higher the satellite cloud fraction is relative to the surface sky cover, the lower (greater) the direct (diffuse) flux becomes. Because these values are of opposite sign, the direct and diffuse flux differences tend to cancel. However, the differences in the direct flux are generally larger than the diffuse flux differences, leading to the overall negative bias in the SRB SW fluxes observed in Figure 4.

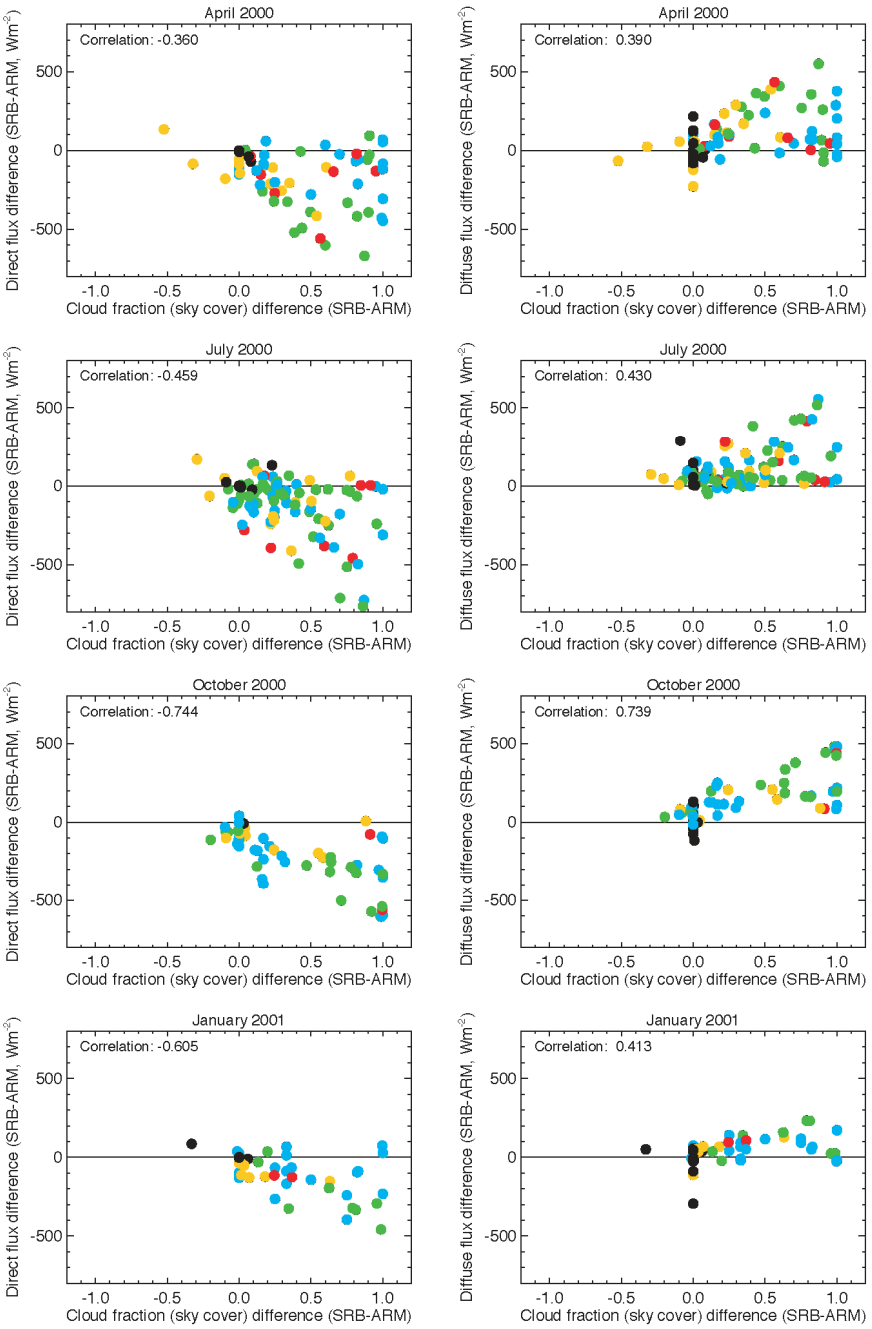

Figure 9. Differences between SRB and ARM direct and diffuse components of the downwelling SW flux as a function of differences in detected cloud cover. (Color coding for sky conditions as shown in Figure 3.)

To determine whether the observed cloud fraction differences are due to errors in the ISCCP data or the surface measurements, we compare the surface data to an independent set of satellite retrievals in Figure 10. Lack of biases in the cloud cover and direct and diffuse fluxes in the unrelated Clouds and the Earth's Radiant Energy System (CERES) Cloud Radiative Swath Edition 2b product relative to SGP

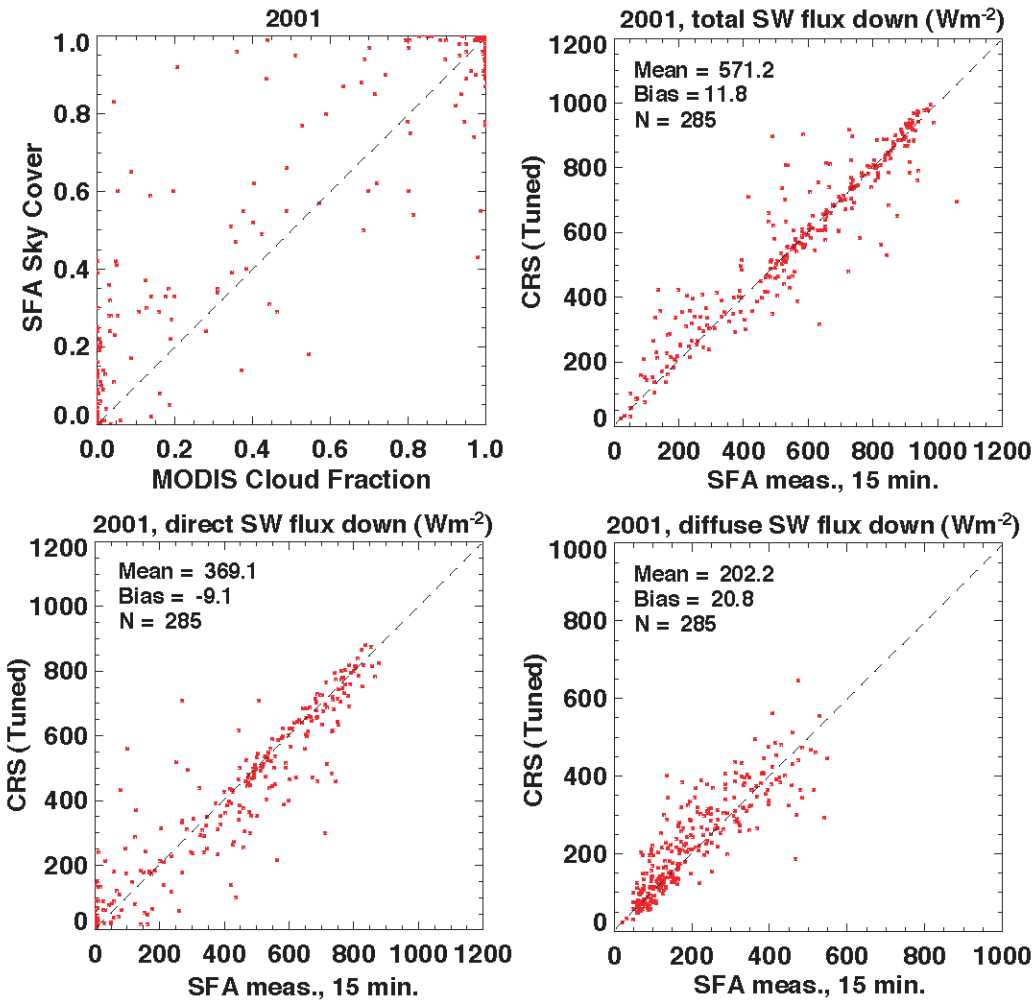

Figure 10. Comparison of CERES CRS products with SGP CF measurements for the entire year of 2001. CERES fluxes are based in part on cloud fraction determined from the moderate resolution imaging spectroradiometer (MODIS). (Note that the axes are reversed in the cloud fraction plot relative to those in the ISCCP-ARM cloud fraction plots.)

CF values implies that the differences observed for the GEWEX Surface Radiation Budget product do not stem from surface measurement errors. (All CERES footprints included here fall within 15 km of the Central Facility.)

Plotting the SRB-ARM SW total flux differences as a time series, as in Figure 11, reveals that the negative bias steadily increased over the years 1998 to 2001. This trend may reflect changes in the amount or type of clouds or changes in the detection of that cloudiness by ISCCP. It may also be related to changes in parameters that influence narrowband-to-broadband or radiance-to-flux conversions, such as surface and cloud properties. Further analysis is required to see whether this trend extends beyond this limited time period or is evident at other locations.

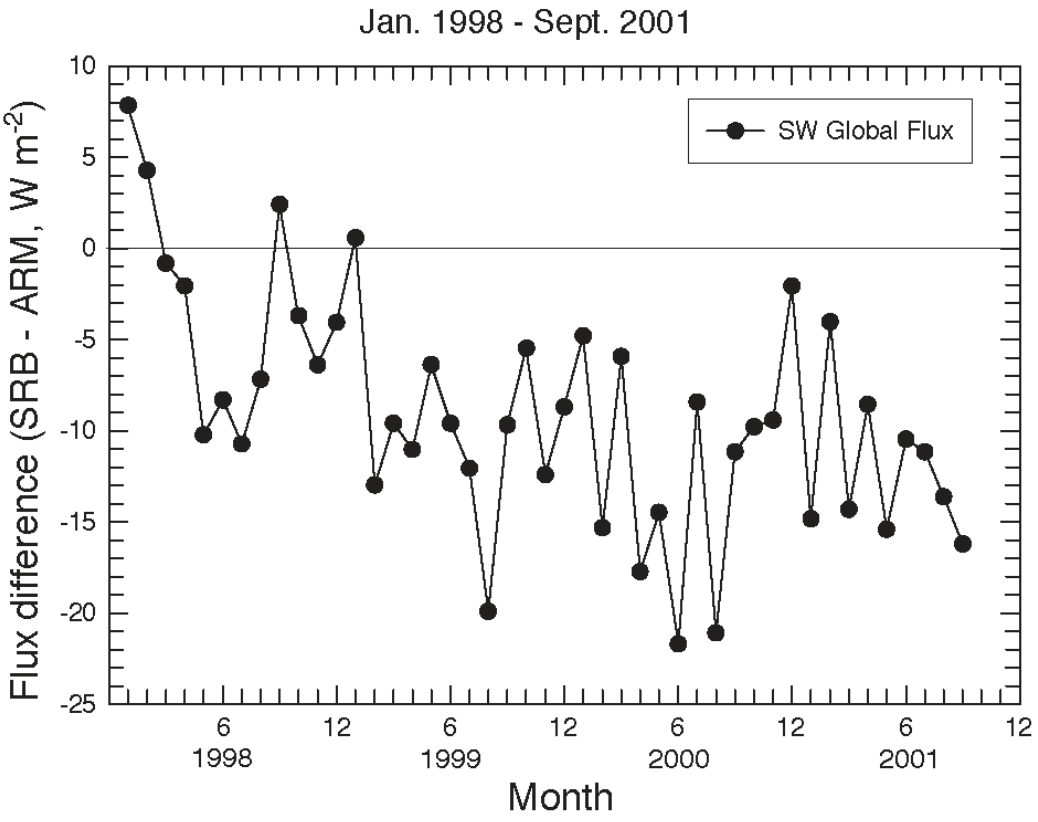

Figure 11. Time series of the difference between the SRB and ARM total downwelling SW flux for the period 1998-2001.

Conclusions

ARM data is a valuable tool for assessing and understanding satellite products. GEWEX Surface Radiation Budget version 2.5 values have been evaluated using measurements from the ARM SGP Central Facility for the months of April, July, and October 2000 and January 2001. Because ARM and ISCCP cloud fractions differ significantly during these months, the SRB direct and diffuse SW fluxes do not agree well with the corresponding ARM values. Over the period of 1998-2001, the SRB total downwelling shortwave flux has decreased relative to ARM measurements. Additional study is required to explain this long-term trend in the differences between GEWEX SRB-estimated and ARM-measured surface fluxes.

Acknowledgments

The authors thank Steven Cox and Taiping Zhang, Analytical Services & Materials, Inc., for their assistance in processing the SRB SW flux data. This work was funded by the Earth-Sun System Science Division of NASA's Science Mission Directorate through the CERES and GEWEX SRB projects. Dr. Long acknowledges the support of the Climate Change Research Division of the U.S. Department of Energy as part of the ARM Program.

References

Long, CN, and TP Ackerman. 2000. "Identification of clear skies from broadband pyranometer measurements and calculation of downwelling shortwave cloud effects." *Journal of Geophysical Research/Journal of Geophysical Research*, 105(D12):15,609-15,626.

Pinker, RT, and I Laszlo. 1992. "Modeling surface solar irradiance for satellite applications on a global scale." *Journal of Applied Meteorology* 31(2):194-211.